J. Fluid Mech. (2010), *vol.* 646, *pp.* 453–470.
doi:10.1017/S002211200999303X

Stochastic coherent adaptive large eddy simulation of forced isotropic turbulence

G. DE STEFANO[1] AND O. V. VASILYEV[2]†

[1]Dipartimento di Ingegneria Aerospaziale e Meccanica, Seconda Università di Napoli, I 81031 Aversa, Italy

[2]Department of Mechanical Engineering, University of Colorado, Boulder, CO 80309, USA

(Received 11 January 2009; revised 22 October 2009; accepted 24 October 2009)

The stochastic coherent adaptive large eddy simulation (SCALES) methodology is a novel approach to the numerical simulation of turbulence, where a dynamic grid adaptation strategy based on wavelet threshold filtering is utilized to solve for the most 'energetic' eddies. The effect of the less energetic unresolved motions is simulated by a model. Previous studies have demonstrated excellent predictive properties of the SCALES approach for decaying homogeneous turbulence. In this paper the applicability of the method is further explored for statistically steady turbulent flows by considering linearly forced homogeneous turbulence at moderate Reynolds number. A local dynamic subgrid-scale eddy viscosity model based on the definition of the kinetic energy associated with the unresolved motions is used as closure model. The governing equations for the wavelet filtered velocity field, along with the additional evolution equation for the subgrid-scale kinetic energy, are numerically solved by means of a dynamically adaptive wavelet collocation method. It is demonstrated that adaptive simulations closely match results from a reference pseudo-spectral fully de-aliased direct numerical simulation, by using only about 1 % of the corresponding computational nodes. In contrast to classical non-adaptive large eddy simulation, the agreement with direct solution holds for the mean flow statistics as well as in terms of energy and enstrophy spectra up to the dissipative wavenumbers range.

1. Introduction

Over the last two decades, starting from the pioneering work by Farge & Rabreau (1988), wavelet decomposition techniques have been successfully applied to study turbulent flows in terms of both *a posteriori* analysis (e.g. Farge, Pellegrino & Schneider 2001; Farge *et al.* 2003; De Stefano, Goldstein & Vasilyev 2005; Okamoto *et al.* 2007) and numerical simulation (Goldstein, Vasilyev & Kevlahan 2005; De Stefano, Vasilyev & Goldstein 2008; Vasilyev *et al.* 2008). Wavelet decomposition has been shown to be an effective tool to decompose fluid motion into an organized coherent part, consisting of a small fraction of the modes that contain the majority of energy and enstrophy of the flow, and an incoherent residual field (e.g. Farge *et al.* 2003; Okamoto *et al.* 2007). As a result, the coherent modes are mostly responsible for the evolution of the turbulence and the wavelet decomposition, thus, provides an efficient physically based method for solving/modelling turbulent flows. This property

† Email address for correspondence: oleg.vasilyev@colorado.edu

of wavelet-based coherent/incoherent velocity field decomposition was utilized by Farge, Schneider & Kevlahan (1999) to introduce the coherent vortex simulation (CVS) method. The evolution of the coherent eddies was proposed to be explicitly simulated by completely discarding the effect of the incoherent part, which was shown to consist of a Gaussian white noise that provides no turbulent dissipation (Farge *et al.* 2001). This way, the number of degrees-of-freedom of the numerical solution was substantially reduced with respect to direct numerical simulation (DNS). However, the computational cost of CVS was closer to DNS than large eddy simulation (LES), mainly because the method relied on physical dissipation and coherent modes were resolved all the way down to the Kolmogorov scale.

In order to overcome the computational constrains of CVS and make the wavelet-based method more feasible, a more comprehensive approach referred to as stochastic coherent adaptive large eddy simulation (SCALES) has been recently proposed by Goldstein & Vasilyev (2004). In the SCALES approach, the formal separation between resolved coherent structures and unresolved eddies is 'shifted' towards the range of more energetic eddies so that the effect of the unresolved motions can no longer be neglected and must be modelled. The introduction of a subgrid-scale (SGS) model makes it possible to further reduce the degrees-of-freedom of the numerical solution and a higher grid compression with respect to CVS is achieved. In fact, the use of a closure model makes the SCALES methodology similar to LES. However, in contrast to standard LES, which is based on linear low-pass filters, SCALES exploits a wavelet-based nonlinear multiscale thresholding filter, which depends on the instantaneous flow realization. Furthermore, the distinctive difference is in the direct coupling of computational grid and SGS model. The method has the ability either to compensate for inadequate SGS dissipation provided by the model by increasing the local resolution and, hence, the level of resolved viscous dissipation or to coarsen the mesh in regions of high SGS dissipation. Both CVS and SCALES approaches have been numerically implemented using the adaptive wavelet collocation method (AWCM), developed by Vasilyev & Bowman (2000), Vasilyev (2003) and Vasilyev & Kevlahan (2005), which allows high-resolution computations to be carried out only in those regions where the turbulent field shows sharp transitions.

Different SGS models, originally developed in the context of LES, have been successfully extended to the SCALES framework. For instance, the dynamic Smagorinsky model, based on the extension of the classical Germano procedure redefined in terms of wavelet thresholding filters, was considered by Goldstein *et al.* (2005). In order to fully exploit the dynamic adaptivity of the method and not to rely on the presence of homogeneous directions to stabilize the numerical calculations (e.g. Lilly 1992), two classes of local dynamic SGS models for SCALES have been proposed recently: a Lagrangian path-line/tube dynamic model (Vasilyev *et al.* 2008) and local one-equation dynamic models based on the SGS turbulent kinetic energy (De Stefano *et al.* 2008).

Until now, the SCALES approach has been almost exclusively tested for incompressible decaying homogeneous turbulence. Due to the decaying nature of the previously studied flows, it was not possible to fully evaluate the method. The objective of this paper is to assess the stability and predictive properties of the SCALES approach for statistically stationary turbulence by performing adaptive LES of forced homogeneous turbulence. Due to the use of adaptive computational mesh by the wavelet solver, it is preferable to introduce forcing directly in physical space. For this reason, in contrast to the classical Fourier forcing that is applied in a narrow

bandwidth of small wavenumbers, we adopt the forcing scheme recently proposed by Lundgren (2003), and extensively studied by Rosales & Meneveau (2005), according to which the force is a simple linear function of velocity.

Two different modelling procedures are tested, namely the global dynamic model introduced in (Goldstein *et al.* 2005) and the localized dynamic kinetic-energy-based model proposed by De Stefano *et al.* (2008). It should be noted that the ultimate objective for the SCALES development is the simulation of turbulent flows of engineering interest. However, this is a subject of future research and is not addressed in this work.

The rest of the paper is organized as follows. The linear forcing assumption is briefly reviewed in § 2. The general features of the SCALES approach to the simulation of forced turbulence, along with the pertinent governing equations, are discussed in § 3. The results of the numerical experiments carried out are presented in § 4 and, finally, some conclusions are given in § 5.

2. Linearly forced isotropic turbulence

The continuity and Navier–Stokes equations for incompressible flow can be written in the forced case as

$$\frac{\partial u_i}{\partial x_i} = 0, \tag{2.1}$$

$$\frac{\partial u_i}{\partial t} + u_j \frac{\partial u_i}{\partial x_j} = -\frac{1}{\rho}\frac{\partial p}{\partial x_i} + \nu \frac{\partial^2 u_i}{\partial x_j \partial x_j} + f_i, \tag{2.2}$$

where ρ and ν are the constant density and kinematic viscosity of the fluid, while f_i stands for the force per unit mass.

Following the idea of Lundgren (2003), we consider the forcing term proportional to the velocity field, $f_i = Q u_i$, where Q is a constant parameter. For historical fairness, it should be noted that a similar forcing was originally studied in Machiels (1997), where a linear force was applied in Fourier space for a given shell of small wavenumbers. However, in this work, as well as in Lundgren (2003) and Rosales & Meneveau (2005), the turbulence is forced uniformly in the entire wavenumbers domain.

The forcing coefficient Q can be expressed in terms of the turbulent flow characteristics. As shown in Lundgren (2003), the balance equation for the kinetic energy, $k = u_i\, u_i/2$, can be written as

$$\frac{\partial k}{\partial t} + u_j \frac{\partial k}{\partial x_j} = -\frac{1}{\rho}\frac{\partial}{\partial x_i}(p\, u_i) + \nu \frac{\partial^2 k}{\partial x_j \partial x_j} - \tilde{\varepsilon} + 2Qk, \tag{2.3}$$

where $\tilde{\varepsilon} = \nu(\partial u_i/\partial x_j)(\partial u_i/\partial x_j)$ stands for the so-called pseudo-dissipation (Pope 2000). By assuming statistically homogeneous turbulence and exploiting the continuity constraint (2.1), the energy equation is rewritten in terms of volume-averaged variables as

$$\frac{\mathrm{d}K}{\mathrm{d}t} = -\langle \tilde{\varepsilon} \rangle + 2QK, \tag{2.4}$$

where $K = \langle k \rangle$ stands for the mean kinetic energy and angular brackets denote volume-averaging. It is worth noting that the turbulent dissipation is usually defined as $\varepsilon = 2\nu S_{ij} S_{ij}$, where $S_{ij} = (\partial u_i/\partial x_j + \partial u_j/\partial x_i)/2$ is the rate-of-strain tensor. However, in the present homogeneous case, for the corresponding mean values it can be

readily shown that $\langle\tilde{\varepsilon}\rangle = \langle\varepsilon\rangle$ (Pope 2000). For this reason, in the following, the mean dissipation can be used instead of the mean pseudo-dissipation.

For statistically steady flow, the energy production rate must equal the dissipation by viscous effects so that, according to (2.4), for the constant forcing parameter it simply holds

$$Q = \frac{\langle\varepsilon\rangle}{2K}. \tag{2.5}$$

This way, the turbulent field is continuously supplied with the amount of energy necessary to keep the total kinetic energy statistically constant in time. Note that fixing the parameter Q is equivalent to prescribing the turbulent time scale since the forcing parameter implicitly sets the eddy turnover time of the turbulence:

$$\tau_{eddy} = \frac{u'^2}{\langle\varepsilon\rangle} = \frac{1}{3Q}, \tag{2.6}$$

where $u' = (2K/3)^{1/2}$ stands for the r.m.s. velocity. Furthermore, the energy spectrum at statistical steady state is insensitive to the initial velocity conditions (e.g. Rosales & Meneveau 2005).

3. Forced turbulence simulation

In this section, after recalling some important features of the wavelet-thresholding-based method, the filtered governing equations are introduced along with the closure models employed in the simulation.

3.1. *Wavelet filtering and adaptive wavelet collocation method*

Wavelet filtering is performed in the wavelet space through wavelet coefficient thresholding. The wavelet filtered velocity is defined by representing the instantaneous turbulent velocity field in terms of wavelet basis functions and retaining only wavelets with significant energy:

$$\overline{u}_i^{>\epsilon}(\boldsymbol{x}) = \sum_{\mathbf{l}\in\mathscr{L}^0} c_{\mathbf{l}}^0 \phi_{\mathbf{l}}^0(\boldsymbol{x}) + \sum_{j=0}^{+\infty}\sum_{\mu=1}^{2^n-1} \sum_{\substack{\boldsymbol{k}\in\mathscr{K}^{\mu,j} \\ |d_{\boldsymbol{k}}^{\mu,j}|>\epsilon\|u_i\|_{WTF}}} d_{\boldsymbol{k}}^{\mu,j}\psi_{\boldsymbol{k}}^{\mu,j}(\boldsymbol{x}). \tag{3.1}$$

In the above decomposition, bold subscripts denote an index in n-dimensional space, e.g. $\boldsymbol{k} = (k_1, \ldots, k_n)$, while $\mathscr{L}^0$ and $\mathscr{K}^{\mu,j}$ are n-dimensional index sets associated with scaling functions at zero level of resolution ($\phi_{\mathbf{l}}^0$) and wavelets of family μ and level j ($\psi_{\boldsymbol{k}}^{\mu,j}$), respectively. Each level of resolution j consists of a family of wavelets $\psi_{\boldsymbol{k}}^{\mu,j}$ having the same scale but located at different positions. The details about the type and shape of the wavelets employed in the SCALES approach can be found in (Goldstein & Vasilyev 2004). When a numerical discretization of the physical domain is introduced, an one-to-one correspondence between grid points and wavelet coefficients is prescribed. Discarding a wavelet, $\psi_{\boldsymbol{k}}^{\mu,j}(\boldsymbol{x})$, whose coefficient $d_{\boldsymbol{k}}^{\mu,j}$ is below a given threshold practically means that u_i has no significant variation at the jth level of resolution in the immediate vicinity of the wavelet's spatial position. Note that the wavelet-based filter is defined by the non-dimensional relative thresholding level ϵ and the wavelet threshold filtering (WTF) norm, $\|\cdot\|_{WTF}$, which determines the absolute (dimensional) scale. This way, different dimensional quantities can be filtered using the same filter defined for the velocity field by (3.1). In this work, the L_2 norm

is assumed as WTF norm and, for homogeneous turbulence, the same scaling is used in all directions, i.e. $\|u_i\|_{WTF} = \langle 2k_{res} \rangle^{1/2}$, where $k_{res} = \overline{u}_i^{>\epsilon}\, \overline{u}_i^{>\epsilon}/2$ stands for the resolved kinetic energy that is the energy associated to the wavelet filtered velocity.

Owing to the one-to-one correspondence between grid points and wavelet coefficients, by applying the above wavelet threshold filtering procedure, only a subset of the available computational nodes is effectively retained in the calculation and the grid is automatically adapted to the flow evolution, being refined in regions of strong variations. This constitutes the core of the adaptive wavelet collocation method (AWCM) developed by Vasilyev (2003) and Kevlahan & Vasilyev (2005). Briefly, the AWCM is an adaptive, variable-order numerical method for solving partial differential equations with localized structures that change their location and scale. Since the computational grid automatically adapts to the solution, both in position and scale, the regions of dynamically important flow features do not need to be known *a priori*. The method is based on second-generation wavelets (Sweldens 1998), which allow the order of the wavelets (and hence of the numerical method) to be varied easily. The derivatives on the adaptive grid are calculated using finite-difference approximations on fixed stencils by exploiting a ghost point approach (Vasilyev & Bowman 2000; Vasilyev 2003). The method has a computational complexity $O(N)$, where N is the number of wavelets (or, equivalently, grid points) retained in the calculation, i.e. those wavelets with significant coefficients plus nearest neighbours, both in position and scale. The time integration scheme is based on a split-step method, where a non-solenoidal velocity field is calculated in the first step and is made divergence free using a pressure projection in the second step. Since pressure and velocity are given at the same grid points, the Laplace operator for the pressure correction step is constructed as the inner product of a downwind gradient operator and an upwind divergence operator, which automatically avoids the odd–even decoupling instability associated with non-staggered grids (Kevlahan & Vasilyev 2005). The numerical results reported in this paper are obtained with sixth-order second-generation wavelets and sixth order finite-difference approximations on symmetric stencils.

The threshold ϵ in WTF definition (3.1) explicitly defines the energy level of the eddies that are resolved and, consequently, controls the importance of the influence of the residual field on the dynamics of the resolved motions. The choice of a sufficiently low threshold eliminates the need to adopt any modelling procedure, since the residual field is not dynamically significant in this case, and the resulting approach can be referred to as wavelet-based DNS (WDNS). The CVS approach (Farge *et al.* 1999) is obtained by choosing the threshold corresponding to de-nosing criteria of Donoho & Johnstone (1994). In this case, the filtered velocity field represents the coherent turbulent flow structures, whose evolution is computed, while the influence of the incoherent background flow is neglected due to its decorrelation with the coherent flow. Finally, when ϵ is chosen to be sufficiently higher than the CVS threshold, only the most energetic coherent structures are resolved, while the effect of the residual flow is modelled. This regime is representative of the SCALES approach. The aforementioned CVS threshold thus stands for the lower threshold limit for the SCALES method. On the other side, the upper limit is dictated by the requirement to resolve dynamically dominant flow structures, and can be empirically determined. The choice of the actual value of ϵ directly controls the relative importance of SGS modelling and computational cost in the SCALES approach. As illustrated in § 3.3, the larger ϵ the higher is the contribution of the SGS dissipation. Also note that the lower levels of SGS dissipation are associated with the increased grid resolution and the larger per cent of the resolved viscous dissipation.

Finally, it should be noted that there is an additional computational cost associated with the use of the adaptive multi-resolution wavelet methodology. Currently, the cost per point is approximately three to five times greater than that one of the corresponding non-adaptive computational method. However, the high compression achieved, which can be as high as 99.5 %, represents a strong acceleration that greatly outweighs this cost. In addition, memory savings associated with the use of the adaptive methodology allow higher resolution numerical simulations for given available computational resources. Further cost improvement is expected for the future implementations, thanks to the recent development of an efficient data structure that takes advantage of the multi-resolution hierarchical structure of the wavelet decomposition (Vasilyev *et al.* 2008).

3.2. *Filtered governing equations*

The SCALES equations, which describe the space–time evolution of the most energetic coherent eddies in the flow, can be formally obtained by applying the wavelet thresholding filter (3.1) to the continuity (2.1) and Navier–Stokes (2.2) equations. The SCALES governing equations for linearly forced incompressible turbulence are written as

$$\frac{\partial \overline{u}_i^{>\epsilon}}{\partial x_i} = 0, \tag{3.2}$$

$$\frac{\partial \overline{u}_i^{>\epsilon}}{\partial t} + \overline{u}_j^{>\epsilon}\frac{\partial \overline{u}_i^{>\epsilon}}{\partial x_j} = -\frac{1}{\rho}\frac{\partial \overline{p}^{>\epsilon}}{\partial x_i} + \nu\frac{\partial^2 \overline{u}_i^{>\epsilon}}{\partial x_j \partial x_j} - \frac{\partial \tau_{ij}}{\partial x_j} + Q\overline{u}_i^{>\epsilon}. \tag{3.3}$$

As a result of the filtering process, the unresolved quantities

$$\tau_{ij} = \overline{u_i u_j}^{>\epsilon} - \overline{u}_i^{>\epsilon}\,\overline{u}_j^{>\epsilon}, \tag{3.4}$$

commonly referred to as SGS stresses, are introduced. The SGS stresses can be thought of representing the effect of unresolved less energetic background flow on the dynamics of the resolved energetic eddies. In order to close the filtered equation (3.3), a SGS model is required to express the unknown stresses (3.4) as a given function of the resolved velocity field. In practice, the isotropic part of the SGS stress tensor can be incorporated by a modified filtered pressure variable, so that only the deviatoric part, hereafter noted with a star, $\tau_{ij}^* = \tau_{ij} - \tau_{kk}\delta_{ij}/3$, is actually modelled. Henceforth, the filtered momentum equation to be solved is

$$\frac{\partial \overline{u}_i^{>\epsilon}}{\partial t} + \overline{u}_j^{>\epsilon}\frac{\partial \overline{u}_i^{>\epsilon}}{\partial x_j} = -\frac{\partial \overline{P}^{>\epsilon}}{\partial x_i} + \nu\frac{\partial^2 \overline{u}_i^{>\epsilon}}{\partial x_j \partial x_j} - \frac{\partial \tau_{ij}^*}{\partial x_j} + Q\overline{u}_i^{>\epsilon}, \tag{3.5}$$

where $\overline{P}^{>\epsilon} = (\overline{p}^{>\epsilon}/\rho) + (\tau_{kk}/3)$. Note that, analogously to LES with non-uniform filter width (Vasilyev, Lund & Moin 1998; Haselbacher & Vasilyev 2003), the governing equations for SCALES (3.5) are derived without considering the commutation error between wavelet filtering and derivative operators. However, this error is significantly reduced by using the adjacent zone, since a significant number of points below the thresholding level is retained in the simulations (e.g. Vasilyev 2003).

The balance equation for the resolved kinetic energy, $k_{res} = \overline{u}_j^{>\epsilon}\,\overline{u}_j^{>\epsilon}/2$, according to (3.5), is the following:

$$\frac{\partial k_{res}}{\partial t} + \overline{u}_j^{>\epsilon}\frac{\partial k_{res}}{\partial x_j} = -\frac{\partial}{\partial x_i}\left[\overline{u}_j^{>\epsilon}\left(\tau_{ij}^* + \overline{P}^{>\epsilon}\delta_{ij}\right)\right] + \nu\frac{\partial^2 k_{res}}{\partial x_j \partial x_j} - \tilde{\varepsilon}_{res} - \Pi + 2Qk_{res}, \tag{3.6}$$

where $\tilde{\varepsilon}_{res} = \nu(\partial \overline{u}_i^{>\epsilon}/\partial x_j)(\partial \overline{u}_i^{>\epsilon}/\partial x_j)$ stands for the resolved pseudo-dissipation. The term $\Pi = -\tau_{ij}^* \overline{S}_{ij}^{>\epsilon}$ represents the SGS dissipation, which is the rate at which energy is

locally transferred from energetic resolved eddies to unresolved residual motions. It is worth noting that the resolved viscous dissipation for SCALES is higher than for classical non-adaptive LES, since small-scale dissipative eddies with significant energy are resolved.

Once volume-averaged, by also exploiting (3.2), (3.6) becomes

$$\frac{\mathrm{d}K_{res}}{\mathrm{d}t} = -\langle\tilde{\varepsilon}_{res}\rangle - \langle\Pi\rangle + 2QK_{res}, \tag{3.7}$$

where $K_{res} = \langle k_{res}\rangle$ is the mean resolved kinetic energy. As for the mean resolved turbulent dissipation, it holds $\langle\tilde{\varepsilon}_{res}\rangle = \langle\varepsilon_{res}\rangle$, where $\varepsilon_{res} = 2\nu\overline{S}_{ij}^{>\epsilon}\overline{S}_{ij}^{>\epsilon}$ and $\overline{S}_{ij}^{>\epsilon} = (\partial\overline{u}_i^{>\epsilon}/\partial x_j + \partial\overline{u}_j^{>\epsilon}/\partial x_i)/2$ stands for the resolved rate-of-strain tensor. For the statistically stationary flow, the SCALES analog of (2.5) becomes

$$Q = \frac{\langle\varepsilon_{res}\rangle + \langle\Pi\rangle}{2K_{res}}. \tag{3.8}$$

In the SCALES approach the resolved kinetic energy content of the flow practically coincides with that one of the corresponding DNS solution so that $K_{res} \cong K$. Therefore, in order to have a solution that matches the DNS results, given the forcing parameter and thus the eddy turnover time of the turbulence, the SGS model must provide the right energy dissipation in order to have $\langle\varepsilon_{res}\rangle + \langle\Pi\rangle \cong \langle\varepsilon\rangle$. That is confirmed by the numerical experiments carried out in this work and discussed in § 4.

3.3. *SGS dynamic model*

The filtered equations (3.5) are closed by using the classical eddy viscosity assumption

$$\tau_{ij}^{*} \cong -2\nu_t\overline{S}_{ij}^{>\epsilon}. \tag{3.9}$$

The turbulent eddy viscosity ν_t is determined according to either the global dynamic model (GDM) proposed by (Goldstein *et al.* 2005) or the localized dynamic kinetic-energy-based model (LDKM) developed in (De Stefano *et al.* 2008).

In the first case, the SGS stress tensor is approximated by

$$\tau_{ij}^{*} \cong -2C\Delta^2\epsilon^2|\overline{\boldsymbol{S}}^{>\epsilon}|\overline{S}_{ij}^{>\epsilon}, \tag{3.10}$$

where $|\overline{\boldsymbol{S}}^{>\epsilon}|^2 = 2\overline{S}_{ij}^{>\epsilon}\overline{S}_{ij}^{>\epsilon}$. When making a comparison with the standard Smagorinsky approach for non-adaptive dynamic LES, the quantity $C\epsilon^2$ should be interpreted as the modified model coefficient, while Δ stands for the equivalent filter size. The group $C\Delta^2\epsilon^2$ is dynamically evaluated during the simulation by introducing a wavelet test filter at twice the threshold, while averaging along homogeneous directions is performed in order to stabilize the numerical solution, so that the model parameter is a function of time only. The details of the GDM procedure can be found in (Goldstein *et al.* 2005), where, in particular, the SGS dissipation was demonstrated to scale with ϵ^2. Note that the GDM results are only reported for comparison purposes to demonstrate that both local and global dynamic models work appropriately in the context of forced turbulence simulation.

In the second case, a modelling mechanism that accounts for the local kinetic energy transfer back and forth between resolved and unresolved eddies is exploited by calibrating the eddy viscosity model coefficient based on the energy level of the residual motions. This level is represented by the SGS kinetic energy

$$k_{sgs} = \frac{1}{2}\left(\overline{u_i u_i}^{>\epsilon} - \overline{u}_i^{>\epsilon}\overline{u}_i^{>\epsilon}\right) = \overline{k}^{>\epsilon} - k_{res}. \tag{3.11}$$

The unknown SGS stress tensor is approximated by the eddy viscosity model (3.9) with the turbulent viscosity defined by taking the square root of k_{sgs} as the velocity scale and the wavelet filter characteristic width Δ as the length scale. Namely, we assume

$$\tau^*_{ij} \cong -2C_\nu \Delta k^{1/2}_{sgs} \overline{S}^{>\epsilon}_{ij}, \tag{3.12}$$

where C_ν stands for a dimensionless model coefficient to be determined. The filter width Δ at a given time instant can be extracted from the knowledge of the wavelet mask used during the simulation.

By exploiting the LDKM procedure, the SGS dissipation rate is approximated as a monotonic function of k_{sgs}, that is,

$$\Pi \cong C_\nu \Delta k^{1/2}_{sgs} |\overline{\boldsymbol{S}}^{>\epsilon}|^2. \tag{3.13}$$

Note that the modelled SGS dissipation increases with the wavelet filtering threshold and can show both signs, thus allowing for the simulation of local energy backscatter. The modelling procedure is completed by incorporating the following model transport equation for the SGS kinetic energy variable (e.g. Ghosal *et al.* 1995):

$$\frac{\partial k_{sgs}}{\partial t} + \overline{u}^{>\epsilon}_j \frac{\partial k_{sgs}}{\partial x_j} = (\nu + \nu_t) \frac{\partial^2 k_{sgs}}{\partial x_j \partial x_j} - \tilde{\varepsilon}_{sgs} + \Pi, \tag{3.14}$$

where $\tilde{\varepsilon}_{sgs}$ stands for the SGS viscous dissipation, that is,

$$\tilde{\varepsilon}_{sgs} = \nu \left(\overline{\frac{\partial u_i}{\partial x_j} \frac{\partial u_i}{\partial x_j}}^{>\epsilon} - \frac{\partial \overline{u}^{>\epsilon}_i}{\partial x_j} \frac{\partial \overline{u}^{>\epsilon}_i}{\partial x_j} \right) = \overline{\varepsilon}^{>\epsilon} - \tilde{\varepsilon}_{res}. \tag{3.15}$$

A further model for this term must be introduced in order for (3.14) to be closed. By using simple scaling arguments, the approximation $\tilde{\varepsilon}_{sgs} = C_\varepsilon \Delta^{-1} k^{3/2}_{sgs}$ is used, with C_ε a dimensionless coefficient. Both the model parameters C_ν and C_ε can be determined as pointwise functions of space and time by exploiting classical dynamic procedures using either a Germano-like or a Bardina-like approach, as discussed in De Stefano *et al.* (2008). In this paper, for the sake of brevity, only the results using the Germano-like approach for the eddy viscosity model and the Bardina one for the SGS viscous dissipation model are presented. The wavelet filtered Navier–Stokes equations (3.5) and the SGS kinetic energy equation (3.14) supplied with the above models stand for a closed system of coupled equations that is solved with the adaptive wavelet collocation method (e.g. Vasilyev & Kevlahan 2002; Kevlahan, Alam & Vasilyev 2007).

Let us stress the important property of the LDKM procedure, namely the presence of the physically based built-in feedback mechanism between the resolved kinetic energy and the SGS kinetic energy through the common term, Π, which acts as energy dissipation in (3.6) and SGS kinetic energy production in equation (3.14). That mechanism automatically stabilizes the numerical solution, as demonstrated by the results presented in the following section. More details about the LDKM approach can be found in De Stefano *et al.* (2008).

4. Numerical experiments

The filtered Navier–Stokes equations (3.5) are solved, along with the SGS energy equation (3.14), in a cubic box with triply periodic boundary conditions. The initial velocity field for the numerical experiments is obtained by wavelet filtering

of a fully de-aliased pseudo-spectral 192^3 DNS statistically steady solution with $Re_\lambda \cong 60$ (De Stefano *et al.* 2005). Due to the finite-difference nature of the adaptive solver, the maximum resolution has been increased in each direction with respect to the spectral DNS case in order not to alter the initial energy content. SCALES is run using a maximum resolution corresponding to 256^3 grid points. However, thanks to the wavelet filtering procedure, only a very low fraction of these points is actually used during the simulation. In particular, the thresholding level $\epsilon = 0.43$ adopted here corresponds to that one already used in the past for simulating flows at comparable Reynolds number (e.g. Goldstein *et al.* 2005).

According to the linear forcing scheme discussed in § 2, the forcing term is evaluated directly in physical space with the forcing parameter $Q = 5.2$ prescribed in order to retain in average the energy content of the initial flow field. Note that the above choice corresponds to fixing the eddy turnover time at $\tau_{eddy} = 0.064$. The simulations are conducted for a temporal range of one hundred eddy turnover times. Diagnostics include the time evolution of energy and energy dissipation, as well as the time-averaged energy spectra. Moreover, we consider the evolutions of the eddy turnover time and the Taylor-scale Reynolds number. The latter is defined as $Re_\lambda = u'\lambda/\nu$, where the Taylor length scale can be evaluated for isotropic turbulence as $\lambda = (15\nu u'^2/\langle\varepsilon\rangle)^{1/2}$ (e.g. Pope 2000).

4.1. *Reference solutions*

In order to build a reference fully de-aliased pseudo-spectral DNS solution, the unfiltered Navier–Stokes equations (2.2) are solved on a 192^3 Fourier grid by exploiting the same method of De Stefano *et al.* (2005). Owing to the moderate Reynolds number, which is in average $Re_\lambda \cong 55$, it holds $k_{max}\eta \cong 1.3$, where $k_{max} = 64$ is the highest resolved wavenumber and η stands for the Kolmogorov length scale. It is worth noting that the Reynolds number is not sufficiently high to allow a clear inertial scaling in the energy spectrum. Furthermore, since the linear forcing acts uniformly in the whole wavenumbers domain, the spectrum does not show any peak, in contrast to what happens for classical low-wavenumber forcing. In fact, the present spectral DNS is fully consistent with one of those conducted by Rosales & Meneveau (2005) at $Re_\lambda \cong 51$.

As further reference, the numerical solution of the wavelet filtered Navier–Stokes equations with no SGS model is considered, i.e. τ_{ij}^* is set to zero in the filtered momentum equation (3.5). Owing to the adaptive nature of the method, the wavelet-based solution is able to react to the lack of the SGS dissipation by increasing the numerical resolution, retaining more computational nodes with respect to the modelled case. However, having prescribed a given wavelet threshold, small-size eddies with small energy cannot be reproduced. Taking the nature of the linearly forced homogeneous turbulence and the ability of the method to automatically increase the resolution, the no-model simulation, after a substantially long transient, reaches the equilibrium with turbulence statistics remarkably close to DNS, including energy and enstrophy spectra. The relatively low cost of the increased resolution with respect to the modelled simulations is due to the moderate Reynolds number of the flow. For higher Reynolds number flows the computational cost of the increased resolution would be substantially higher and a SGS model would be required to make simulations practical. The results presented in the next section demonstrate how the introduction of a model makes it possible to mimic the energy dissipation provided by the unresolved small scales, thus recovering DNS statistics with coarser resolution.

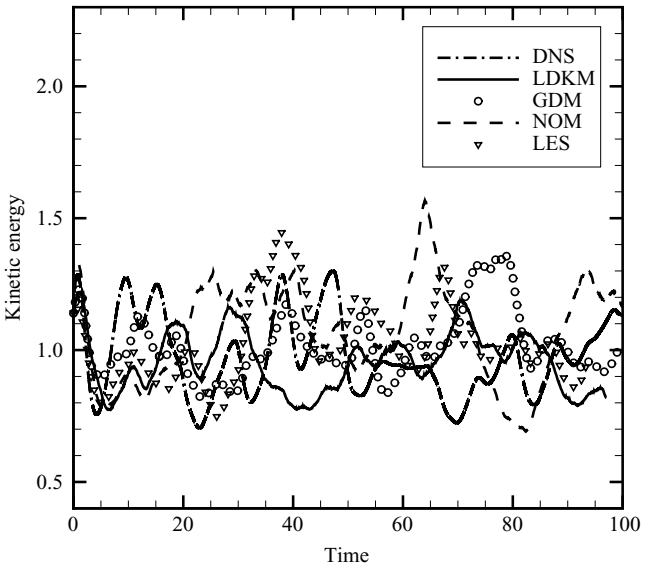

FIGURE 1. Resolved kinetic energy, normalized by the time-averaged DNS energy, for SCALES with localized dynamic kinetic-energy-based model (LDKM) and global dynamic model (GDM). The pseudo-spectral DNS, no-model (NOM), and non-adaptive dynamic LES solutions are shown as reference. The time is normalized by the theoretical eddy turnover time.

Finally, in order to highlight the difference between SCALES and classical non-adaptive LES, the present results are compared to the LES solution obtained on a regular 64^3 grid using the same wavelet-based code without grid adaptation. This LES calculation is supplied with the global dynamic Smagorinsky eddy viscosity model.

4.2. *SCALES solutions*

The kinetic energy evolution for the two different SCALES solutions is illustrated in figure 1, compared with the reference pseudo-spectral DNS solution. In this as well as in the other figures the time is normalized by the theoretical eddy turnover time that is $(3Q)^{-1}$. The energy level is normalized by the time-averaged DNS energy while the volume averaging is performed in physical space. As one can see, the wavelet-based solutions are able to match the averaged DNS energy level. The major part of the energy content of the flow is captured by a limited number of wavelets. In fact, the SCALES solutions use in average only 0.5 % of the available 256^3 wavelets, as demonstrated in figure 2, where the percentage of active wavelets is reported. The present grid compression is in agreement with previous studies on decaying homogeneous turbulence. The achieved compression corresponds to retaining about 1 % of the 192^3 Fourier modes used for de-aliasing in the reference spectral DNS, according to the 3/2 rule (e.g. De Stefano *et al.* 2005). Moreover, by making a comparison with the no-model solution, it seems evident that the introduction of a SGS model makes it possible to substantially reduce the number of computational nodes involved in the simulation. Since the computational complexity of the wavelet-based method is $O(N)$, the savings in terms of computational cost of the calculations directly link to the achieved grid compression (Kevlahan & Vasilyev 2005). In particular, considering that the sixth order AWCM code is about three to five times slower per grid point than pseudo-spectral code, the compression factor of

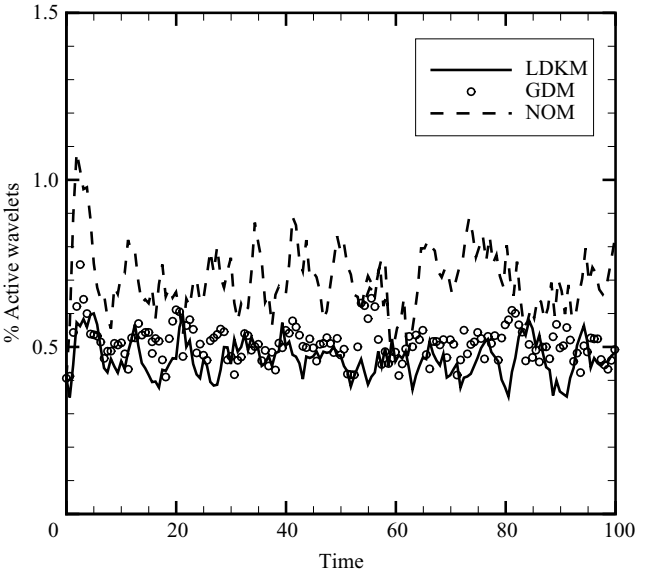

FIGURE 2. Percentage of active wavelets for SCALES with LDKM and GDM models. The no-model solution is shown as reference. Labels and time normalization as in figure 1.

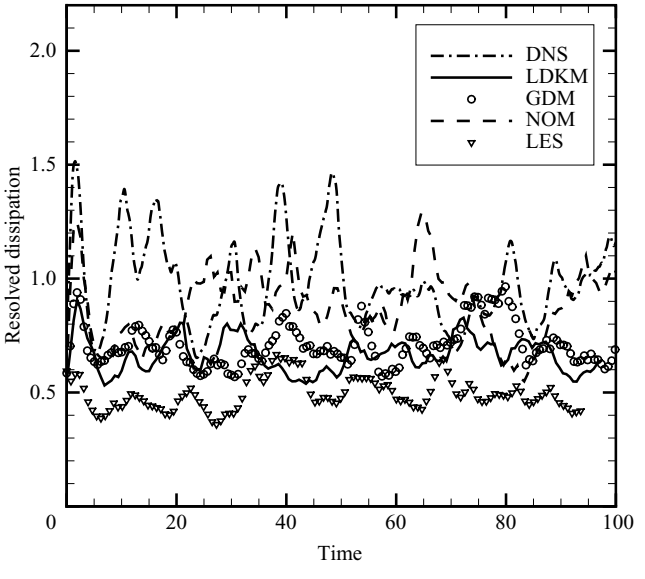

FIGURE 3. Resolved dissipation, normalized by the time-averaged DNS dissipation, for SCALES with LDKM and GDM models. The pseudo-spectral DNS, no-model and non-adaptive dynamic LES solutions are shown as reference. Labels and time normalization as in figure 1.

100 obtained for LDKM thus represents an acceleration that is about 25 times with respect to pseudo-spectral DNS.

The effectiveness of the model is confirmed by analysing the resolved viscous dissipation and the total dissipation, i.e. the sum of resolved and modelled SGS dissipation, reported in figures 3 and 4, respectively. The model is able to provide the

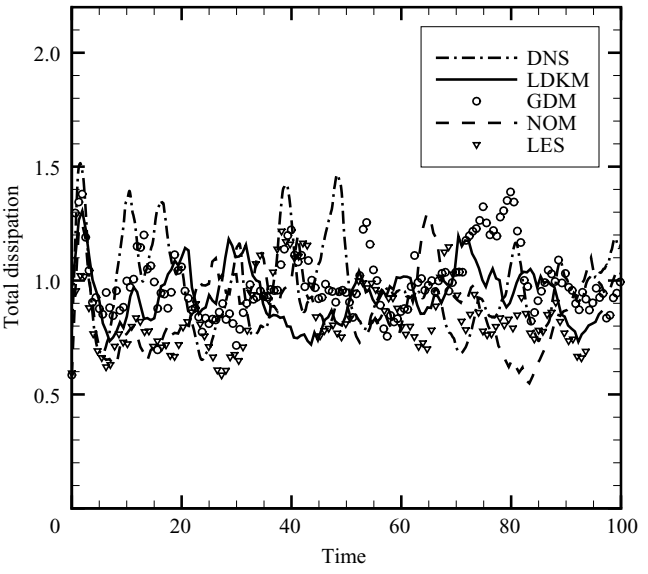

FIGURE 4. Total dissipation, normalized by the time-averaged DNS dissipation, for SCALES with LDKM and GDM models. The pseudo-spectral DNS, no-model and non-adaptive dynamic LES solutions are shown as reference. Labels and time normalization as in figure 1.

right amount of energy dissipation in order to match the DNS viscous dissipation. It should be emphasized that, since the linear forcing acts all the way down to the dissipative scales, this fact also indirectly confirms the good agreement in the evolution of the resolved kinetic energy. The same does not hold for non-adaptive dynamic LES, also reported in the figure, for which the resolved viscous dissipation is much lower. In this case, the SGS model can only partly compensate such loss and the total dissipation does not match DNS. Note that since the forcing parameter Q is constant, according to (3.8), the total dissipation and the resolved kinetic energy are not independent measures of the simulation skill.

In fact, a distinctive feature of the SCALES methodology is the ability to simulate the dynamically important energetic small-scale motions in a turbulent flow field. That is confirmed in the present linearly-forced case by inspection of the time-averaged energy and enstrophy spectra, reported in figures 5 and 6, respectively. By making a comparison with spectra corresponding to the wavelet filtered DNS, which stands for the ideal solution, one can conclude that SCALES is able to represent highest wavenumber modes in a way that non-adaptive LES is unable to do. In the non-adaptive case there is also an overestimation of the energy associated to the largest scales. Good agreement between no-model (NOM) and wavelet filtered DNS spectra is not surprising. As demonstrated by Vasilyev *et al.* (2008) for freely decaying turbulence and confirmed here in the forced case, thanks to the adaptive nature of the method, in absence of modelled dissipation, the energy is transferred to smaller scales all the way down to Kolmogorov scale, where it is dissipated by viscous stresses. As illustrated in figure 2, the number of active wavelets for the NOM solution is higher with respect to the modelled cases, and the simulation tends towards the computationally expensive CVS regime.

Moreover, the fact that both averaged kinetic energy and averaged total dissipation are almost identical to corresponding DNS data also allows us to make a comparison

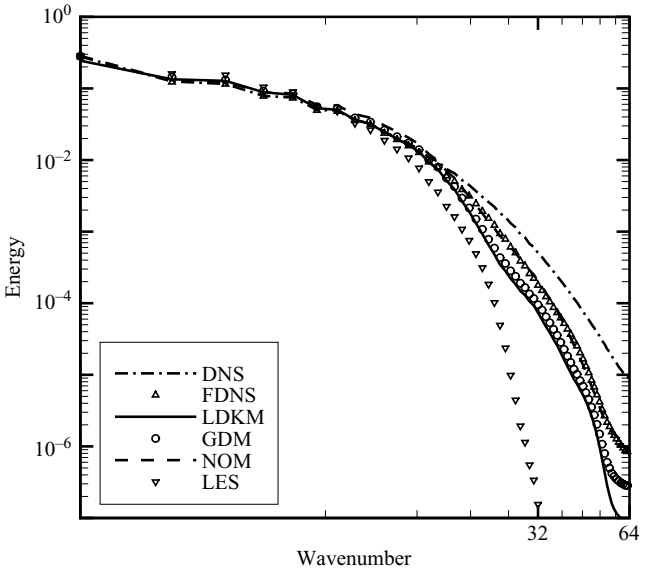

FIGURE 5. Time-averaged energy spectra, normalized by the time-averaged DNS energy, for SCALES with LDKM and GDM models. The pseudo-spectral DNS, wavelet filtered DNS (FDNS), no-model and non-adaptive dynamic LES solutions are shown as reference. The wavenumber variable is normalized by the size of the cubic computational domain. Labels as in figure 1.

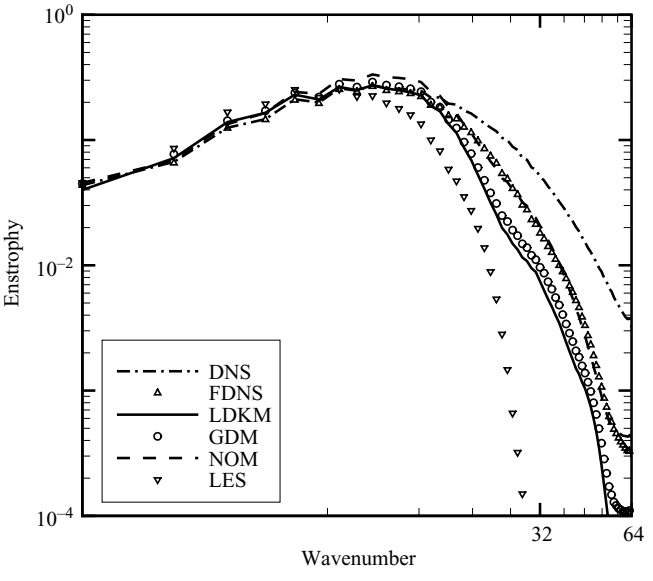

FIGURE 6. Time-averaged enstrophy spectra, normalized by the time-averaged DNS dissipation, for SCALES with LDKM and GDM models. The pseudo-spectral DNS, wavelet filtered DNS (FDNS), no-model and non-adaptive dynamic LES solutions are shown as reference. The wavenumber variable is normalized by the size of the cubic computational domain. Labels as in figure 1.

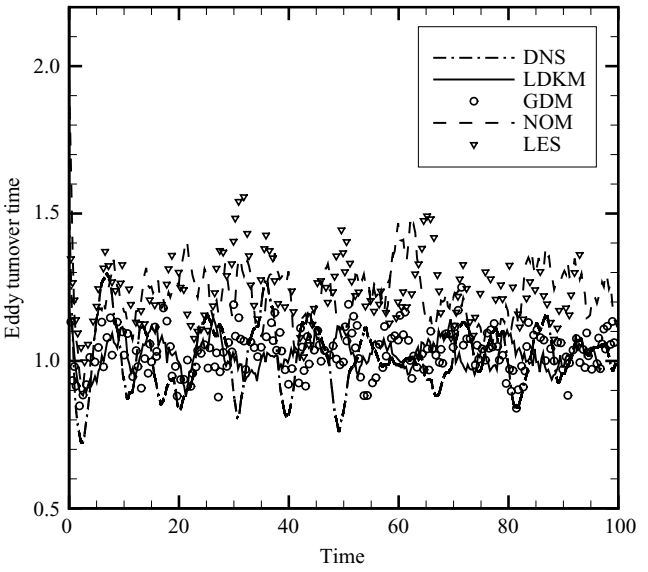

FIGURE 7. Eddy turnover time $\tau_{eddy} = u'^2/\langle\varepsilon\rangle$, normalized by the theoretical value $(3Q)^{-1}$, for SCALES with LDKM and GDM models. The pseudo-spectral DNS, no-model and non-adaptive dynamic LES solutions are shown as reference. Labels and time normalization as in figure 1.

for other statistical quantities of interest. This is a unique feature of the SCALES approach that is distinctively different from standard non-adaptive LES, where often such direct comparison with DNS cannot be made. However, in order to make a meaningful comparison, the statistics that involve the level of energy dissipation must be redefined in terms of the total dissipation. This is illustrated, for instance, for the eddy turnover time and the Taylor-scale Reynolds number in figures 7 and 8, respectively. Once again, the SCALES results match almost perfectly DNS data. Finally, as an example of high-order statistics, in figures 9 and 10 the skewness and the kurtosis of a velocity-derivative component are depicted, respectively.

The present results demonstrate the effectiveness and efficiency of the SCALES methodology in the forced case. The two different models tested agree well in the present homogeneous case, while the localized model is expected to perform better for non-homogeneous turbulent flows. Solving a subgrid energy transport equation allows proper representation of the energy transfer between resolved and SGS motions, both forward and backscatter. In order to quantify backscatter, the percentage of adaptive grid points where negative SGS dissipation occurs ($C_v < 0$) and the fraction of SGS dissipation due to inverse energy transfer are shown in figure 11 for a reduced time interval. It appears that energy backscatter involves about 31 % of the active grid points. Moreover, in the LDKM framework, the SGS to resolved kinetic energy ratio, $\langle k_{sgs}\rangle/\langle k_{res}\rangle$, can be interpreted as a measure of the turbulence resolution of the simulation. After the short initial transient, this ratio has been found to tend towards a statistically constant value that is about 6 %. Let us also note that, in contrast to what experienced for decaying turbulence by De Stefano *et al.* (2008), the SCALES solution is practically insensitive to the initial value of the k_{sgs} variable in the present forced case. Finally, the localized model is expected to work even better for non-homogeneous as well as higher Reynolds number flows.

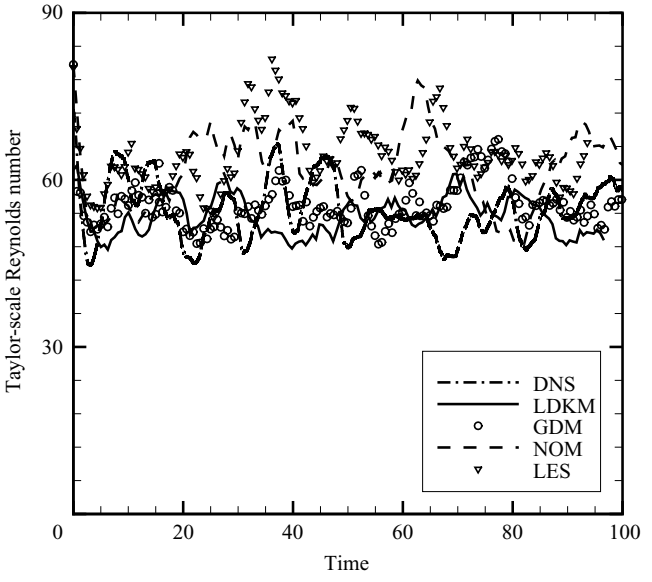

FIGURE 8. Taylor-scale Reynolds number for SCALES with LDKM and GDM models. The pseudo-spectral DNS, no-model and non-adaptive dynamic LES solutions are shown as reference. Labels and time normalization as in figure 1.

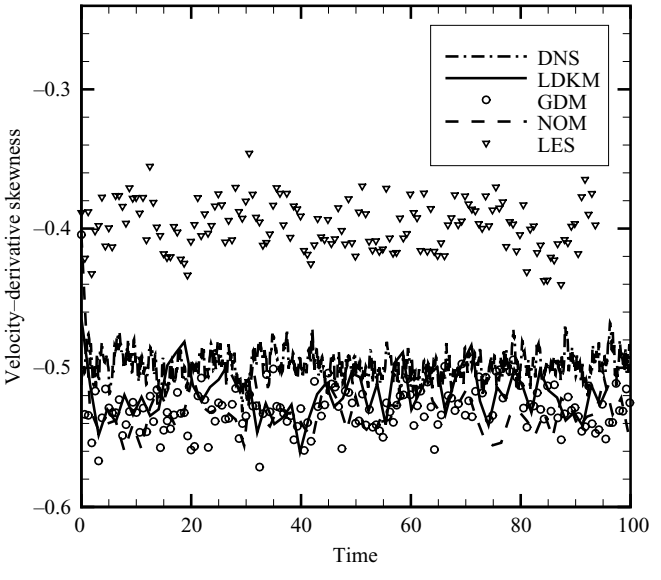

FIGURE 9. Velocity derivative skewness for SCALES with LDKM and GDM models. The pseudo-spectral DNS, no-model and non-adaptive dynamic LES solutions are shown as reference. Labels and time normalization as in figure 1.

5. Conclusions

Adaptive large eddy simulations of linearly forced isotropic turbulence are successfully performed. The energy transfer between resolved and residual motions is either mimicked or directly ensured by solving an additional transport model equation

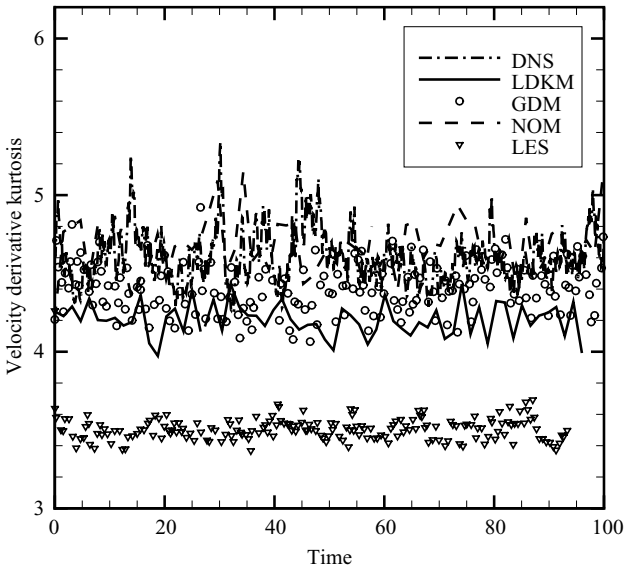

FIGURE 10. Velocity derivative kurtosis for SCALES with LDKM and GDM models. The pseudo-spectral DNS, no-model and non-adaptive dynamic LES solutions are shown as reference. Labels and time normalization as in figure 1.

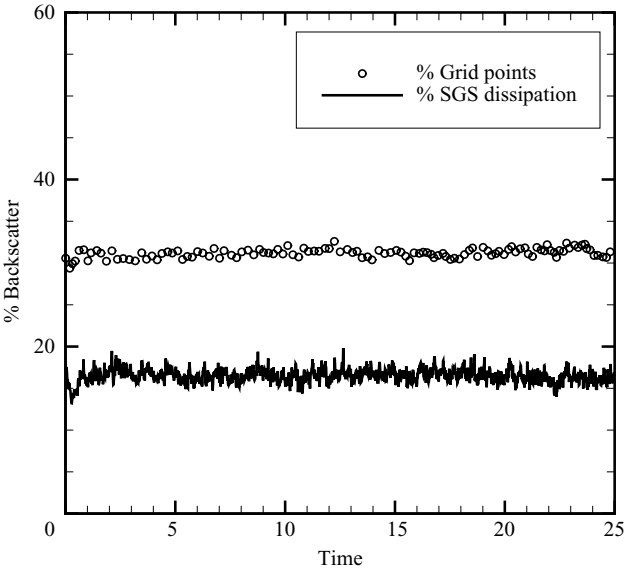

FIGURE 11. Percentage of grid points with energy backscatter and fraction of negative SGS dissipation for SCALES with LDKM model. Time normalization as in figure 1.

for the SGS kinetic energy. The energy-based dynamic modelling procedure controls backscatter-induced instabilities over long-time integration.

The SCALES solutions match the filtered DNS with a very high grid compression with respect to the non-adaptive case. The energy level and the energy and enstrophy spectra are comparable to reference pseudo-spectral DNS. The same holds for other relevant statistics. The model provides the right amount of energy dissipation as

demonstrated by suitably evaluating the corresponding statistics in terms of the total dissipation, resolved plus SGS dissipation.

The present study demonstrates that the SCALES method supplied with either the localized dynamic energy-based or the global dynamic model works for statistically steady flows. This work represents a further step in the development of the wavelet-based methodology in order to apply it to the simulation of high Reynolds number turbulent flows of scientific and engineering interest. In fact, the adaptive-gridding strategy makes the method more complete with respect to the classical non-adaptive approach, being almost fully free from subjective specifications.

This work was supported by the Department of Energy (DOE) under grant No. DE-FG02-05ER25667 and the National Science Foundation (NSF) under grant No. CBET-0756046. In addition G.D.S. was partially supported by a research grant from Regione Campania (L.R.5).

REFERENCES

De Stefano, G., Goldstein, D. E. & Vasilyev, O. V. 2005 On the role of subgrid scale coherent modes in large eddy simulation. *J. Fluid Mech.* **525**, 263–274.

De Stefano, G., Vasilyev, O. V. & Goldstein, D. E. 2008 Localized dynamic kinetic energy-based models for stochastic coherent adaptive large eddy simulation. *Phys. Fluids* **20** (4), 045102.1–045102.14.

Donoho, D. L. & Johnstone, I. M. 1994 Ideal spatial adaptation via wavelet shrinkage. *Biometrika* **81**, 425–455.

Farge, M., Pellegrino, G. & Schneider, K. 2001 Coherent vortex extraction in 3d turbulent flows using orthogonal wavelets. *Phys. Rev. Lett.* **87** (5), 054501-1–054501-4.

Farge, M. & Rabreau, G. 1988 Transformee en ondelettes pour detecter et analyser les structures coherentes dans les ecoulements turbulents bidimensionnels. *C. R. Academie des Sciences de Paris* **307** (serie II), 1479–1486.

Farge, M., Schneider, K. & Kevlahan, N. 1999 Non-Gaussianity and coherent vortex simulation for two-dimensional turbulence using an adaptive orthogonal wavelet basis. *Phys. Fluids.* **11** (8), 2187–2201.

Farge, M., Schneider, K., Pellegrino, G., Wray, A. A. & Rogallo, R. S. 2003 Coherent vortex extraction in three-dimensional homogeneous turbulence: comparison between CVS-wavelet and POD-Fourier decompositions. *Phys. Fluids.* **15** (10), 2886–2896.

Ghosal, S., Lund, T. S., Moin, P. & Akselvoll, K. 1995 A dynamic localization model for large-eddy simulation of turbulent flows. *J. Fluid Mech.* **286**, 229–255.

Goldstein, D. E. & Vasilyev, O. V. 2004 Stochastic coherent adaptive large eddy simulation method. *Phys. Fluids* **16** (7), 2497–2513.

Goldstein, D. E., Vasilyev, O. V. & Kevlahan, N. K.-R. 2005 CVS and SCALES simulation of 3D isotropic turbulence. *J. Turbul.* **6** (37), 1–20.

Haselbacher, A. & Vasilyev, O. V. 2003 Commutative discrete filtering on unstructured grids based on least-squares techniques. *J. Comput. Phys.* **187** (1), 197–211.

Kevlahan, N. K.-R., Alam, J. M. & Vasilyev, O. V. 2007 Scaling of space–time modes with Reynolds number in two-dimensional turbulence. *J. Fluid Mech.* **570**, 217–226.

Kevlahan, N. K.-R. & Vasilyev, O. V. 2005 An adaptive wavelet collocation method for fluid-structure interaction at high Reynolds numbers. *SIAM J. Sc. Comput.* **26** (6), 1894–1915.

Lilly, D. K. 1992 A proposed modification of the Germano subgrid-scale closure method. *Phys. Fluids* A **4**, 633–635.

Lundgren, T. S. 2003 Linearly forced isotropic turbulence. *Annu. Res. Briefs,* 461–473.

Machiels, L. 1997 Predictability of small-scale motion in isotropic fluid turbulence. *Phys. Rev. Lett.* **79**, 3411–3414.

Okamoto, N., Yoshimatsu, K., Schneider, K., Farge, M. & Kaneda, Y. 2007 Coherent vortices in high resolution direct numerical simulation of homogeneous isotropic turbulence: a wavelet viewpoint. *Phys. Fluids* **19** (115109), 1–13.

Pope, S. B. 2000 *Turbulent Flows*. Cambridge University Press.

Rosales, C. & Meneveau, C. 2005 Linear forcing in numerical simulations of isotropic turbulence: physical space implementations and convergence properties. *Phys. Fluids* **17**, 1–8.

Sweldens, W. 1998 The lifting scheme: a construction of second generation wavelets. *SIAM J. Math. Anal.* **29** (2), 511–546.

Vasilyev, O. V. 2003 Solving multi-dimensional evolution problems with localized structures using second generation wavelets. *Intl J. Comput. Fluid Dyn.,* Special issue on High-resolution methods in Computational Fluid Dynamics **17** (2), 151–168.

Vasilyev, O. V. 2008 Adaptive LES methodology for turbulent flow simulations. *Tech. Rep.* DE-FG02-05ER25667-3. U.S. Department of Energy.

Vasilyev, O. V. & Bowman, C. 2000 Second generation wavelet collocation method for the solution of partial differential equations. *J. Comput. Phys.* **165**, 660–693.

Vasilyev, O. V., De Stefano, G., Goldstein, D. E. & Kevlahan, N. K.-R. 2008 Lagrangian dynamic SGS model for stochastic coherent adaptive large eddy simulation. *J. Turbul.* **9** (11), 1–14.

Vasilyev, O. V. & Kevlahan, N. K.-R. 2002 Hybrid wavelet collocation – Brinkman penalization method for complex geometry flows. *Intl J. Numer. Methods Fluids* **40**, 531–538.

Vasilyev, O. V. & Kevlahan, N. K.-R. 2005 An adaptive multilevel wavelet collocation method for elliptic problems. *J. Comput. Phys.* **206** (2), 412–431.

Vasilyev, O. V., Lund, T. S. & Moin, P. 1998 A general class of commutative filters for LES in complex geometries. *J. Comput. Phys.* **146**, 105–123.